

# Control of time-dependent biological processes by temporally patterned input

VLADIMIR BREZINA, IRINA V. OREKHOVA, AND KLAUDIUSZ R. WEISS

Department of Physiology and Biophysics, and the Fishberg Research Center in Neurobiology, Box 1218, Mount Sinai School of Medicine, 1 Gustave L. Levy Place, New York, NY 10029

Edited by Michael V. L. Bennett, Albert Einstein College of Medicine, Bronx, NY, and approved July 9, 1997 (received for review February 5, 1997)

**ABSTRACT** Temporal patterning of biological variables, in the form of oscillations and rhythms on many time scales, is ubiquitous. Altering the temporal pattern of an input variable greatly affects the output of many biological processes. We develop here a conceptual framework for a quantitative understanding of such pattern dependence, focusing particularly on nonlinear, saturable, time-dependent processes that abound in biophysics, biochemistry, and physiology. We show theoretically that pattern dependence is governed by the nonlinearity of the input–output transformation as well as its time constant. As a result, only patterns on certain time scales permit the expression of pattern dependence, and processes with different time constants can respond preferentially to different patterns. This has implications for temporal coding and decoding, and allows differential control of processes through pattern. We show how pattern dependence can be quantitatively predicted using only information from steady, unpatterned input. To apply our ideas, we analyze, in an experimental example, how muscle contraction depends on the pattern of motorneuron firing.

When measuring input–output relations in biological systems, it is often observed that the magnitude of the output depends not just on the magnitude of the input, but also on its temporal pattern—its arrangement in time. The pattern of firing of a neuron—to cite the most notable example—is found to modulate seemingly every activity-dependent variable, including the spread of the electrical activity within the neuron (1), transmitter and hormone release (2–8), postsynaptic integration of the signal (9), levels of second messengers (8, 10, 11), as well as more complex consequences such as synaptic plasticity (12–14), regulation of ion-channel complements (15–17), neurite growth and motility (11, 18), and gene expression (11, 19, 20). Another output variable that is modulated by neuronal firing pattern is muscle contraction (21–25). Fig. 1 shows a dramatic example of this in a well known preparation, the accessory radula closer (ARC) neuromuscular system of *Aplysia* (26–29). Even though all five motorneuron firing patterns shown contain the same mean density of spikes, they produce very different peak, and more importantly mean, levels of contraction. Further examples of pattern dependence are found in biochemical systems, for instance in response to different frequencies of oscillation in levels of hormones and intracellular second messengers (30, 31).

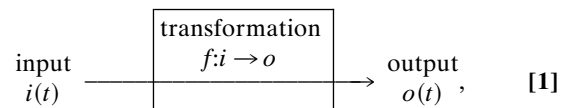
Temporal pattern dependence is thus a very common phenomenon; indeed, it will be one of our conclusions here that it is necessarily ubiquitous. However, beyond the basic observations of its presence, its study has been limited by the lack of a conceptual framework with which to quantitatively define, understand, and predict pattern dependence in biological systems. In this paper, we shall develop such a framework. We

shall then use the experimentally advantageous ARC-muscle system to illustrate and test our ideas.

## Formalization of the Problem

To be able to see under what circumstances pattern dependence can, or cannot, arise, we must first pose the question, and define “pattern” and “pattern dependence,” more precisely. (Nevertheless, from the mathematical standpoint, our presentation and notation in this paper is informal, aiming at an intuitive sketch of the main points rather than complete precision. More technical matters are noted in *Appendices A1–A14*.)

Consider an arbitrary input–output relation



where  $i$ , and therefore  $o$ , varies with time,  $t$ . Our question becomes: what forms of  $f$  are sufficient or necessary for patterns in  $i$  to affect such properties of  $o$  as its peak ( $\bar{o}$ ) and mean ( $\langle o \rangle$ ) amplitude?

Clearly, pattern is a property of an interval of time; we can suppose  $i$  to be periodic and study one period,  $P$ . For simplicity, we shall in this paper concern ourselves only with steady-state pattern dependence, after  $i$  has been applied sufficiently long for  $o$  to be invariant in successive periods. Let  $I = \int_P i dt$ , the “amount” of  $i$  in  $P$ , and  $\langle i \rangle = I/P$ , the mean  $i$ . Similarly,  $\langle o \rangle = (1/P) \int_P o dt$ . Any particular input waveform  $\mathcal{F}_x$  [i.e., the sequence  $i_x(t)$ ,  $t \in P$ ] is completely defined by  $\langle i_x \rangle$  and the distribution of  $I_x$  over  $P$ —the pattern. Both properties will affect  $o$ . Given only one input waveform or waveforms differing in both properties, with  $f$  unknown, the effect of pattern is indeterminate (see *Appendix A1*). [This has obvious experimental implications (**A2**).]

To isolate the effect of pattern, we therefore consider further only waveforms with the same  $\langle i \rangle$ , which differ only in pattern. In particular, we shall use sets of waveforms of the sort shown in Fig. 1 *A* and *C*, where each waveform  $\mathcal{F}_x$  concentrates the same  $I > 0$  into a single block of  $t_x = \langle i \rangle / F_x$  occupying a different fraction  $0 < F_x \leq 1$  of  $P$  (i.e.,  $F$  is the “duty cycle”). Such waveforms are a natural representation of a variety of biological patterns—in Fig. 1, the grouping of neuronal spikes into bursts—and can serve as elementary constituents of more complex waveforms. (Square waveforms of this sort are also used in most experimental work.) Our qualitative conclusions will be applicable to patterns more generally (even irregular patterns: see **A14**), but this subset will serve as a test case for which we shall perform the analysis of pattern dependence in quantitative terms (**A3**).

It is convenient to always include in our set of waveforms the special waveform  $\mathcal{F}_0$  with  $F_0 = 1$ ,  $i_0 = \langle i \rangle$ —steady input with

The publication costs of this article were defrayed in part by page charge payment. This article must therefore be hereby marked “advertisement” in accordance with 18 U.S.C. §1734 solely to indicate this fact.

© 1997 by The National Academy of Sciences 0027-8424/97/9410444-6\$2.00/0 PNAS is available online at <http://www.pnas.org>.

This paper was submitted directly (Track II) to the *Proceedings* office. Abbreviation: ARC, accessory radula closer.

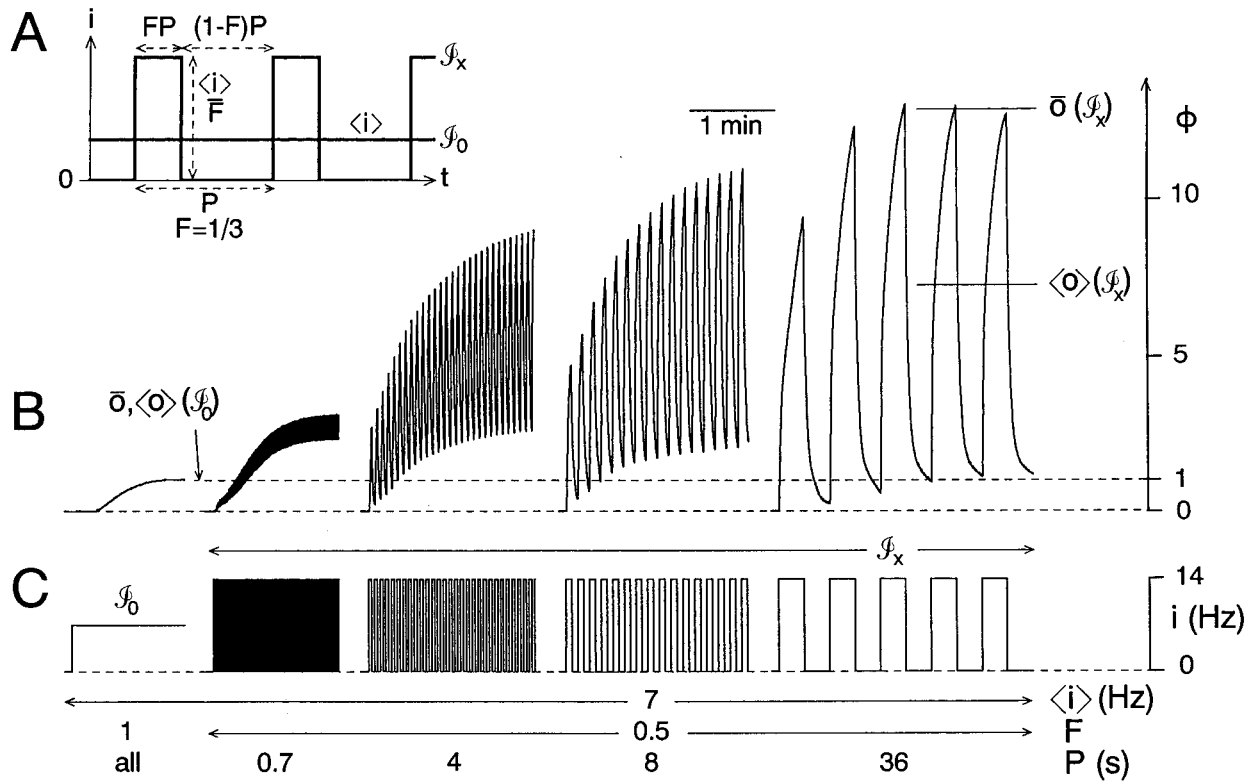


FIG. 1. Pattern and pattern dependence: definitions and examples. (A) Specification of the input waveforms used throughout this work.  $t$ , time;  $i$ , input amplitude;  $\langle i \rangle$ , mean  $i$ ;  $P$ , period;  $F$ , duty cycle;  $\mathcal{I}_0$ , unpatterned waveform of steady input at  $i = \langle i \rangle$ ;  $\mathcal{I}_x$ , a patterned waveform of three times higher input for one-third of the time. (B) Dependence of contraction of the ARC muscle of *Aplysia* on (C) the pattern of motoneuron firing. Experiments were done as in (28, 29). Motoneuron B15 [(26); B15 was used in all experiments presented in this paper; results with B16 were similar] was intracellularly stimulated to fire spikes [individual spikes were driven by separate brief current injections (28), not shown] in the desired pattern, always of the form in A. The firing frequency was taken as the input variable  $i$  and contraction amplitude as the output variable  $o$  (A13). Contractions were isotonic and unloaded; length was monitored with an isotonic transducer.  $\bar{o}$ , peak contraction;  $\langle o \rangle$ , mean contraction. With steady, unpatterned firing (waveform  $\mathcal{I}_0$ ), the contraction reaches the steady state  $\bar{o}(\mathcal{I}_0) = \langle o \rangle(\mathcal{I}_0)$  (Left); with patterned firing (waveforms  $\mathcal{I}_x$ ), it reaches different values  $\bar{o}(\mathcal{I}_x)$  and  $\langle o \rangle(\mathcal{I}_x)$ , as indicated for the rightmost pattern. By Eq. 2, normalizing the values for  $\mathcal{I}_x$  by that for  $\mathcal{I}_0$  establishes the scale of absolute pattern dependence  $\Phi$ , shown on the right of B.

no pattern. In this case, we can write the ratios of the output with patterned input to that with steady, unpatterned input,

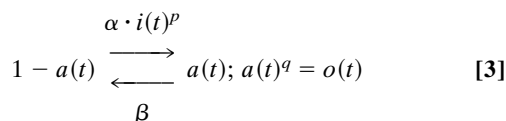
$$\Phi_{\bar{o}}(x, \langle i \rangle) = \frac{\bar{o}(\mathcal{I}_x)}{\bar{o}(\mathcal{I}_0)} \quad \text{and} \quad \Phi_{\langle o \rangle}(x, \langle i \rangle) = \frac{\langle o \rangle(\mathcal{I}_x)}{\langle o \rangle(\mathcal{I}_0)}, \quad [2]$$

for the absolute dependence  $\Phi$  of the peak ( $\bar{o}$ ) and mean ( $\langle o \rangle$ ) output on the pattern  $x$  imposed on mean input  $\langle i \rangle$ . Generally, of course,  $\bar{o}(\mathcal{I}_0) = \langle o \rangle(\mathcal{I}_0)$  (A4), and, since  $\langle o \rangle(\mathcal{I}_x) \leq \bar{o}(\mathcal{I}_x)$ ,  $\Phi_{\langle o \rangle} \leq \Phi_{\bar{o}}$ . All of this is indicated graphically in Fig. 1.

We find that the mean output is pattern independent ( $\Phi_{\langle o \rangle} = 1$ ) if and only if  $f$  is a linear transformation (A5 and A6). If  $f(i) = \text{constant}$ ,  $\Phi_{\bar{o}} = 1$  also. In any case, as long as  $f$  is instantaneous, the value of  $P$  is immaterial.

### Properties of Biologically Important Transformations.

To actually compute  $\Phi$ , we must specify  $f$ . We shall now specify  $f$  that is itself time dependent (A4), implicit in the differential equation describing the kinetic schema



(where  $0 \leq a \leq 1$ ;  $\alpha, \beta, p, q$ , constants;  $q = 1, 2, 3 \dots$ ) (A7). Rather than producing  $o$  directly,  $i$  now controls the rate of a reaction that produces  $o$ . This is a natural way to think of

many biological mechanisms, and schema 3 is representative of schemata used throughout biophysics, biochemistry, and physiology (32–38). Such schemata share three important properties that are a universal feature of real biological processes: nonlinearity, saturability, and time dependence that can be described by a characteristic time constant (A8). Since it will be these properties that determine our qualitative conclusions, these again will be applicable well beyond the exact form of schema 3, which is just one particular form specified for the purposes of quantitative analysis.

### Properties of Pattern Dependence

Given any  $f$  and any input waveform, we can compute  $\Phi$ . This can always be done numerically. However, for our canonical waveforms as input to the simple  $f$  given by schema 3, we can obtain analytical solutions, because we can explicitly integrate the differential equation involved (A9). This yields the time course of  $a$ , and thus of  $o$ , as they rise and fall during the two phases of the pattern (see Fig. 2F). The requirement that in the dynamical steady state of the system the rise and fall must be equal fixes the absolute elevation of the output waveform, and so gives  $\bar{o}$  and  $\langle o \rangle$ . Thus, in the dynamical steady state reached with patterned  $i$ , just as in the true steady state reached with steady  $i$ , we are able to convert knowledge of the kinetics of  $o$  into knowledge of its absolute amplitude.

Thus, we can derive analytical expressions giving  $\Phi_{\bar{o}}$  and  $\Phi_{\langle o \rangle}$  for any pattern  $x$  in terms of  $\alpha, \beta, p, q$ , and  $\langle i \rangle$  (A9). Because  $f$  is time dependent, we must now include  $P$  in the specification of  $x$ . With our waveforms, any pattern  $x$  is uniquely defined by

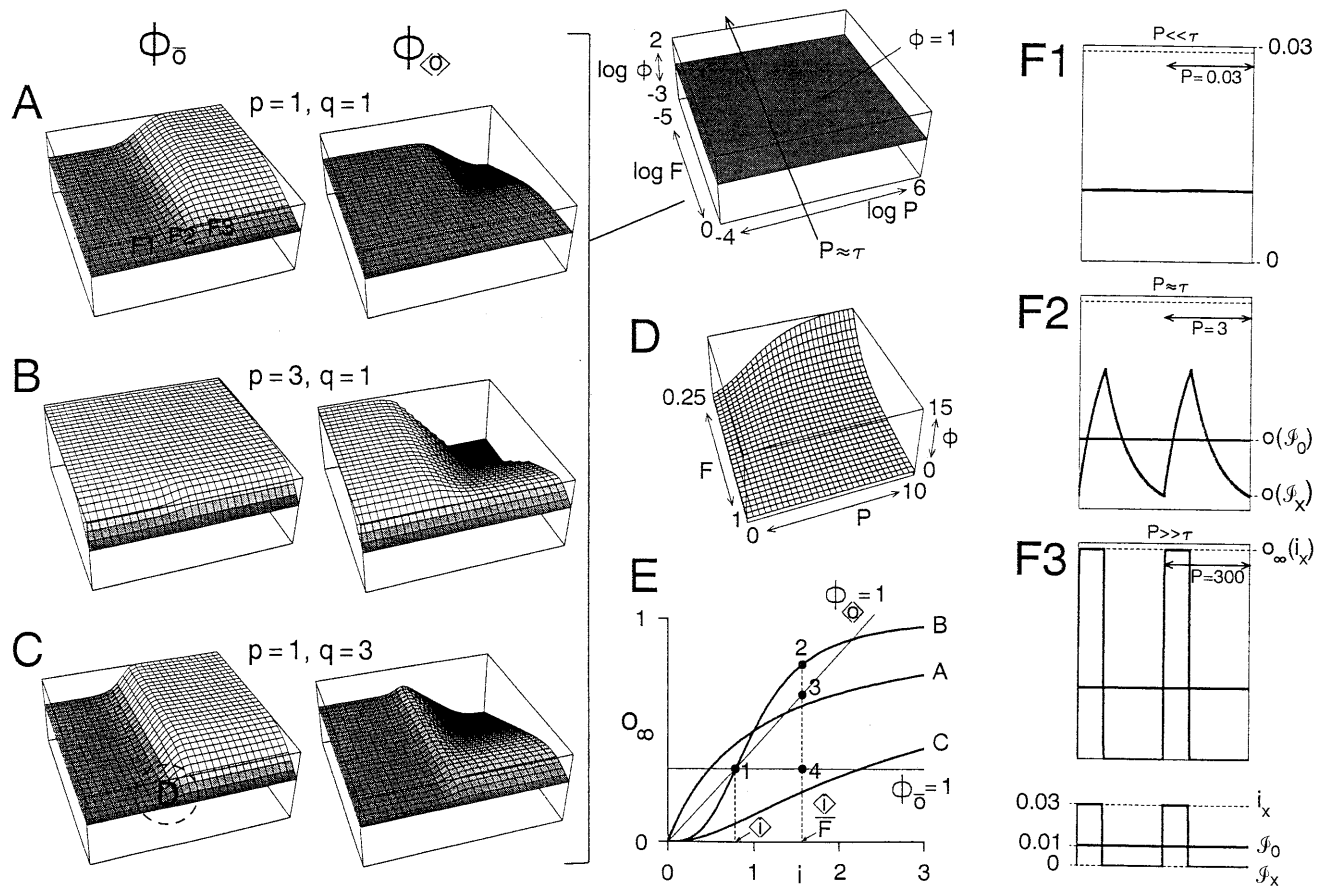


FIG. 2. Theoretical properties of pattern dependence, with transformation  $f$  given by schema 3. (A–C) For three representative cases,  $\Phi_{\bar{o}}$  (Left) and  $\Phi_{\phi}$  (Right) are plotted as functions of the pattern ( $F, P$ ), using Eqs. 6 and 7 in A9. Coordinates as well as locations of the line  $P \approx \tau$  (A8) and surface  $\Phi = 1$  are indicated in the upper middle diagram.  $\Phi = 1$  is represented in medium gray,  $\Phi > 1$  lighter, and  $\Phi < 1$  darker. In all cases  $\alpha, \beta = 1$ ,  $p$  and  $q$  are as indicated, and  $\langle i \rangle = 0.01$  (A) or 0.25 (B and C). These values of  $\langle i \rangle$  were chosen to give  $o_{\infty}(\langle i \rangle) \approx 0.01$  and  $\tau \approx 1$  in all three cases. (D) Linear plot of the circled region in C. (E) The steady-state  $f: o_{\infty} - i$  relations for the three cases in A–C (A10). For  $P \gg \tau$ ,  $\Phi_{\bar{o}}$  and  $\Phi_{\phi}$  may be computed from such relations as follows. As F3 shows,  $\bar{o}(\mathcal{J}_x) = o_{\infty}(i_x)$  and  $\langle o \rangle(\mathcal{J}_x) = F o_{\infty}(i_x)$ , and of course  $\bar{o}(\mathcal{J}_0) = \langle o \rangle(\mathcal{J}_0) = o_{\infty}(\langle i \rangle)$ . Then, from Eq. 2,  $\Phi_{\bar{o}} = o_{\infty}(i_x)/o_{\infty}(\langle i \rangle)$  and  $\Phi_{\phi} = F o_{\infty}(i_x)/o_{\infty}(\langle i \rangle) = F \Phi_{\bar{o}}$ . Setting  $\Phi_{\bar{o}} = 1$  and  $\Phi_{\phi} = 1$  yields equations for the two lines shown. For any particular  $\langle i \rangle$  and  $F$  [here illustrated for  $\langle i \rangle$  on curve B and  $F = 0.5$ , so that  $i_x = 2\langle i \rangle$ ], defining the points 1–4 as shown and writing  $o_{\infty,1}$  for the  $o_{\infty}$  value at point 1, etc., we see that  $\Phi_{\bar{o}} = o_{\infty,2}/o_{\infty,1} = o_{\infty,2}/o_{\infty,4}$  and  $\Phi_{\phi} = F o_{\infty,2}/o_{\infty,1} = o_{\infty,2}/o_{\infty,3}$ . ( $\Phi$  is much smaller here than in A–C because  $\langle i \rangle$  is much larger.)  $\Phi$  can thus be computed even from a purely empirical  $o_{\infty} - i$  relation. In this theoretical case, of course, we know the precise equivalent general expressions for  $\Phi$  (A10). (F) Time courses of  $o$  at the three locations indicated in A—i.e., the solutions (A9) of schema 3 (Eq. 5) with  $\alpha, \beta, p, q = 1$  (since  $q = 1$ , these are also the time courses of  $a$ ), for the input waveforms  $\mathcal{J}_0$  and  $\mathcal{J}_x$  with  $\langle i \rangle = 0.01$ ,  $F = 1/3$ ,  $i_x = 3\langle i \rangle$  (Bottom), when  $P \ll \tau$  (F1),  $P \approx \tau$  (F2), and  $P \gg \tau$  (F3).

the pair ( $F, P$ ), allowing  $x$  to be plotted in two dimensions and  $\Phi$  in the third (A3). This is what we have done in Figs. 2A–C and 3C; Figs. 3E and 4 show sections at a single  $F$ . (In Figs. 2A–C and 4, extended log scales are used to emphasize the asymptotic behavior at extremes, but, as the linear plot in Fig. 2D shows, only fairly small, physiological changes in  $F$  and  $P$  are in fact needed to change  $\Phi$  substantially.)

As  $f$  is nonlinear, we expect pattern dependence. However—and this is the key point—the nonlinearity only appears on time scales longer than  $\tau$ , the time constant of  $f$  (A8). The input pattern exists on time scales shorter than  $P$ . Only when  $P > \tau$ , so that the nonlinearity and the pattern overlap and interact, does the pattern dependence become expressed (A6).

This can be seen in Fig. 2A–C, which are plots of the surfaces of  $\Phi_{\bar{o}}$  and  $\Phi_{\phi}$  for three representative cases. In the  $P$  direction, each plot is divisible into two regions of distinct  $\Phi$ , above and below  $P \approx \tau$ . [In the  $F$  direction,  $\Phi(F = 1) = 1$  by definition for all  $P$  (front edge); pattern dependence becomes expressed as  $F$  decreases.] The characteristic pattern dependence seen in each region can be understood by examining the limiting values that  $\Phi$  tends to when  $P \gg \tau$  or  $P \ll \tau$ , when  $f$ , in effect, becomes time independent again, and  $\Phi$  ceases to vary with  $P$ . Typical time courses of  $o$  when  $P \gg \tau$ ,  $P \approx \tau$ , and  $P \ll \tau$  are shown in Fig. 2F.

When  $P \gg \tau$ ,  $f$  becomes, relative to the time scale of the input pattern, infinitely fast;  $o$  relaxes instantaneously to its new steady-state value,  $o_{\infty}$ , whenever  $i$  changes (Fig. 2F3); the nonlinearity in  $f$  is always fully developed. Then pattern dependence is fully expressed, and its character and magnitude can be found simply by examining the nonlinearity of the steady-state  $f$ —the standard  $o_{\infty} - i$  “dose-response” relation (shown for the three cases in Fig. 2E). In other words, for  $P \gg \tau$ ,  $\Phi$  can be computed—even without kinetic information or indeed any specific model for  $f$ —from just the steady-state output that is reached with steady, unpatterned input of different amplitudes [for details see Fig. 2E (legend) and A10]. In agreement with our earlier result,  $\Phi_{\bar{o}}$  is represented in the  $o_{\infty} - i$  plot by a horizontal line through  $\langle i \rangle$ ,  $\Phi_{\phi} = 1$  by a sloping line through 0 and  $\langle i \rangle$  (Fig. 2E). Upward departure of the  $o_{\infty} - i$  relation from these lines gives “positive” pattern dependence ( $\Phi > 1$ ; greater output with grouped input), downward departure “negative” pattern dependence ( $\Phi < 1$ ; greater output with dispersed input). In Fig. 2A–C, these are shown in lighter and darker tones, respectively.

We note, first, that  $\Phi$  greatly depends on  $\langle i \rangle$ . At different values of  $\langle i \rangle$ , the same pattern will have very different quantitative, and in some cases even qualitative, effects.

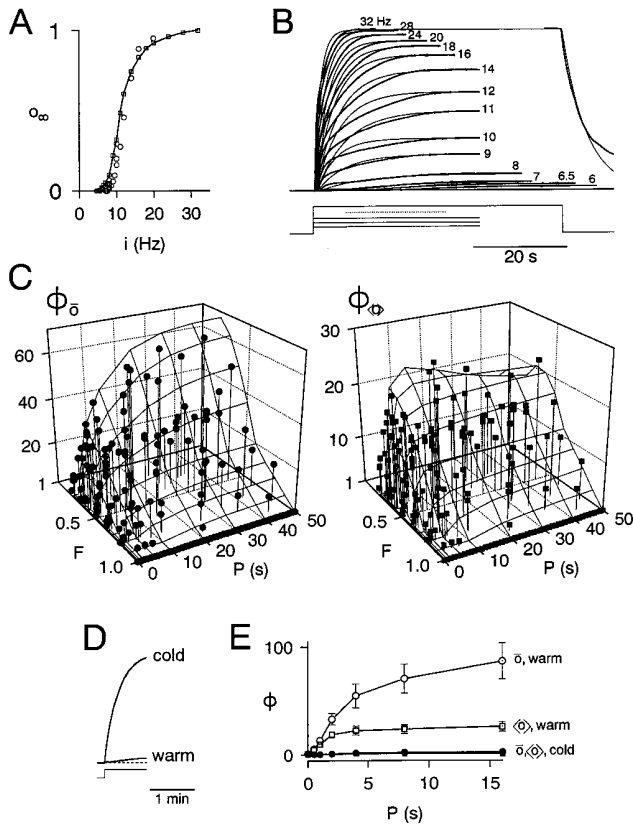


FIG. 3. Experimental analysis of pattern dependence in the *Aplysia* ARC-muscle system. (A and B) Contraction kinetics and  $o_{\infty}$ - $i$  relations (from the experiment in B and two others) obtained with steady, unpatterned motorneuron firing (schematically indicated under B). To summarize the data for the purposes of computation, we fitted the kinetics, at each  $i$ , with a delay  $d(i)$ , then a single-exponential rise with time constant  $\tau(i)$ , to the steady-state amplitude  $o_{\infty}(i)$  (thin, smooth curves in B). Though the actual kinetics are clearly more complex, this form appeared to provide the most simple yet reasonably adequate empirical description of the data. (C)  $\Phi_{\bar{o}}$  and  $\Phi_{\omega}$  predicted from the values obtained from A and B (mesh; computed using the same strategy as in A9) and experimentally measured (scatter points; steady-state measurements as in Fig. 1 B and C). The measured values are from 11 preparations, which gave surfaces of  $\Phi$  of similar shape but different absolute amplitude. The values from each preparation were therefore scaled so as to normalize the reference value  $\Phi(F = 0.5, P = 10 \text{ s})$  to the mean from all preparations ( $\Phi_{\bar{o}}, 27 \pm 19 \text{ SD}$ , range 13–75;  $\Phi_{\omega}, 14 \pm 9 \text{ SD}$ , range 6–37). The mean  $\langle i \rangle$  was 5.7 Hz ( $\pm 1.2 \text{ SD}$ , range 4–8); the same value was used in the theoretical computations. The mean deviation of the experimental points from the predicted surface is 3.4 for  $\Phi_{\bar{o}}, 1.0$  for  $\Phi_{\omega}$  ( $n = 132$ , values for  $F = 1$  excluded). (D) Cooling the preparation (here from 20.3 to 14.9°C; unpatterned firing at 4 Hz) greatly increases contraction amplitude. (E) Concomitantly, cooling greatly reduces  $\Phi$ . Means  $\pm$  SEM from four preparations (not normalized) first at 20–21.1°C, then 14.9–15°C.  $\langle i \rangle = 4$ –5.5 Hz;  $F = 0.25$ . [The experiments in Figs. 1 B and C and 3 A–C were done at the “warm” temperatures. All temperatures used are in the physiological range for *Aplysia* (40).]

Qualitatively, as the  $o_{\infty}$ - $i$  relation is always strictly increasing (for  $p > 0$ ), we always find  $\Phi_{\bar{o}} > 1$  no matter what  $\langle i \rangle$  we choose. But the finite amount of  $a$  in schema 3, resulting in downward curvature of the  $o_{\infty}$ - $i$  relation, gives  $\Phi_{\omega} < 1$ . Thus, interestingly, the saturating dose-response relations that abound in biology inherently impose “negative” pattern dependence of mean output. “Positive” pattern dependence, requiring a region of upward curvature in the  $o_{\infty}$ - $i$  relation, becomes superimposed when  $p > 1$  or  $q > 1$ , but only over a limited range of low  $\langle i \rangle$ . Both kinds of pattern dependence are observed experimentally (2–8, 11, 19, 20). At the crayfish opener neuromuscular junction, for example, summation of excitatory junctional potentials leading to muscle contraction

shows “positive” pattern dependence, while induction of long-term potentiation shows “negative” pattern dependence (39).

When  $P \ll \tau$ ,  $f$  becomes, relative to the time scale of the input pattern, infinitely slow; within any particular period,  $o$  does not sense changes in  $i$  at all (Fig. 2FI); thus  $\bar{o} = \langle o \rangle$  and  $\Phi_{\bar{o}} = \Phi_{\omega}$ . The important question is whether, in the steady state, the output stabilizes at the same  $\langle o \rangle$  regardless of pattern. If it does, then  $\Phi_{\bar{o}} = \Phi_{\omega} = 1$ —the output is pattern independent. This is true if and only if, when  $P \ll \tau$ ,  $f$  becomes linear (A11). With schema 3, this happens only when  $p = 1$  (Fig. 2A and C). When  $p \neq 1$ ,  $\Phi_{\bar{o}} = \Phi_{\omega} \neq 1$  (Fig. 2B). This can be thought of as the result of inclusion, within  $f$ , of a preceding input-output step with instantaneous nonlinearity (A12). Thus, two forms of  $f$  with similar  $o_{\infty}$ - $i$  relations and therefore similar pattern dependence when  $P \gg \tau$ , such as schema 3 with  $p = 1$ ,  $q > 1$  and  $p > 1$ ,  $q = 1$ , may nevertheless give very different pattern dependence as  $P$  decreases depending on exactly how their nonlinearities depend on time.

### Analysis of Pattern Dependence in a Real System

We can now see how well these principles apply in a real experimental case of pattern dependence, that in the *Aplysia* ARC-muscle system. We take the frequency of motorneuron firing as the input variable  $i$  and contraction amplitude as the output variable  $o$  (A13). Then, from just contraction parameters obtained with steady, unpatterned firing—now not only the final amplitude but also the kinetics of development of the contraction (Fig. 3 A and B)—we are able to compute, in the same way as for the theoretical cases, predictions of the complete surfaces of both  $\Phi_{\bar{o}}$  and  $\Phi_{\omega}$ . These predictions prove to be very accurate when they are then tested with actual patterned firing (Fig. 3C). Pattern dependence indeed develops when  $P > \tau$ , of the order of several seconds. As expected from the curvature of the  $o_{\infty}$ - $i$  relation (Fig. 3A), we see strong “positive” pattern dependence, with hints of underlying “negative” pattern dependence of  $\Phi_{\omega}$  at small  $F$  and large  $P$ . As in the theoretical cases, the balance between “positive” and “negative” pattern dependence shifts toward the latter if  $\langle i \rangle$  is increased toward saturation of the  $o_{\infty}$ - $i$  relation.

Interestingly, the same shift can be achieved, without changing  $\langle i \rangle$ , by contraction-enhancing modulation. The effect of temperature (a physiological variable for a poikilotherm such as *Aplysia*) is shown in Fig. 3 D and E; modulatory transmitters (27–29) have similar though lesser effects. (In this context, we note that our framework predicts another important way in which pattern dependence can be modulated, namely by a change in  $\tau$ .)

Two further points are worth emphasizing. First, rather than using schema 3, or indeed postulating *a priori* any precise kinetic model for  $f$ , in this case we simply described the observed kinetics with arbitrary, purely empirical functions. Thus there is nothing essential about the particular form of schema 3; our analysis applies generally. If we know the kinetics—no matter how complex—with which the output develops in response to steady input  $i^*$ , we can always predict  $\Phi$  for the pattern with  $i_x = i^*$ . If we do not have a precise model for  $f$ , we simply assume, as we did in this case, that the kinetics are the same whenever  $i^*$  occurs, whether steadily or as part of a pattern. That is, we assume that the kinetics depend purely on  $i$ , and not, for example, on  $o$  as well. This is a reasonable starting assumption, and indeed it holds for schema 3 and many similar models. An experimental test of the predicted  $\Phi$  is then a test of this assumption: for the ARC muscle in Fig. 3C, it appears valid. Of course, if we formulate a precise model for  $f$ , perhaps incorporating a different assumption, again  $\Phi$  can be predicted and tested. Thus, pattern dependence can be used, experimentally as well as theoretically, to discriminate between different kinetic models.

Second, the analysis applies to any input-output relation, without requiring knowledge of intermediate steps, which may be, as in the ARC-muscle case, many and complex.

**Significance of Biological Pattern Dependence**

In this paper, then, we have developed a conceptual framework for a quantitative understanding of temporal pattern dependence in biological processes. These concepts have both retrospective and prospective utility. Where pattern dependence has been demonstrated [e.g., with the patterns of neuronal firing (1–25) or oscillating hormone levels (30, 31)] they allow prediction of the properties of the underlying mechanisms. Three other areas that come to mind where temporal pattern is well known to be important are activity-dependent determination and maintenance of muscle properties (41), clinical pharmacokinetics (31, 42), and massed vs. spaced training in experimental psychology (43, 44). But beyond the known cases, temporal patterns are ubiquitous in biology (30, 45–47). In addition to many different kinds of neuronal firing patterns (48–51), diverse biochemical oscillations (30) and intracellular Ca<sup>2+</sup> spikes and waves (30, 52–54) are well known. Time-dependent, nonlinear reactions and transformations are universal. And, whenever a patterned variable acts through such a reaction, the output can be predicted to be pattern dependent in the way we have described.

Of course, many patterns arise primarily from the need to time, phase and synchronize activity *vis-à-vis* other processes or the external world (48–51, 55–57). Even then, pattern dependence of the output of any reaction that inputs the patterned variable will, at least, be an automatic consequence of the existence of such patterns. More interestingly, however, pattern dependence may provide a mechanism by which different patterns are detected and decoded. One important case is the decoding of information encoded in temporal spike patterns in the brain (58–60). Our analysis constrains the properties a process should possess to be able to decode specific patterns. Conversely, given a particular process, it constrains the set of patterns that can be meaningful, in the sense of being distinguishable from other patterns. For example, patterns cannot be differentiated on the basis of  $P$  when  $P \gg \tau$  or  $P \ll \tau$ ; thus any process that is to accomplish this must have  $\tau \approx P$ . And, if  $f$  becomes linear when  $P \ll \tau$ , all patterning or even irregular variability on time scales  $\ll \tau$  is irrelevant (A14).

Finally, differential control of multiple processes may even be the primary role of some patterns. Fig. 4 shows how different processes can be tuned, by virtue of their different time constants, to respond preferentially to different patterns of the same input variable. By varying the input pattern, one or another process can be selected. Already, experimental examples of this have been reported. In the crayfish opener neuromuscular system that we mentioned earlier, for instance, bursts of motoneuron firing contract the muscle without inducing long-term potentiation, whereas steady firing at the same mean frequency has the converse effect (39). Similarly, the extra dimension of temporal pattern may help explain how different signals acting through a common set of processes (e.g., several hormones all acting via intracellular Ca<sup>2+</sup> or cAMP in the same cell) can yet have specific effects (52–54, 61, 62). Clearly, when considering biological variables, temporal pattern is a dimension that should not be neglected.

**Appendix**

**A1.** We test for pattern dependence of  $\langle o \rangle$ , for instance, by asking whether there exists a function  $g$  such that, simultaneously for each given input waveform,

$$\int_P f(i) dt = g\left(\int_P i dt\right), \quad [4]$$

or equivalently  $\langle o \rangle = g(\langle i \rangle)$ —i.e., can pattern be disregarded? If  $g$  does not exist—i.e., some  $\langle i \rangle$  corresponds to more than one

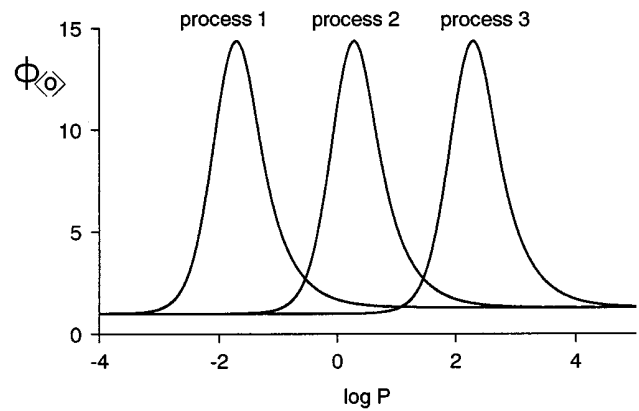


FIG. 4. Different processes can be tuned to respond to different patterns of the same input variable. This is, essentially, a section through the  $\phi_{\langle o \rangle}$  surface in Fig. 2C (thus  $p = 1, q = 3, \langle i \rangle = 0.25$ ) at  $F = -3$  for three processes with time constants two orders of magnitude apart: process 1,  $\alpha = 400, \beta = 1,000$ ; process 2,  $\alpha = 4, \beta = 10$ ; process 3,  $\alpha = 0.04, \beta = 0.1$ . “Windows” of pattern dependence such as these are observed experimentally (11, 19, 20).

$\langle o \rangle$ — $\langle o \rangle$  is pattern dependent. If  $g$  exists—i.e., no  $\langle i \rangle$  corresponds to more than one  $\langle o \rangle$ — $\langle o \rangle$  is pattern independent or, trivially, there is only one waveform with that particular  $\langle i \rangle$ , so it necessarily corresponds to just one  $\langle o \rangle$ .

**A2.** As a consequence of A1, pattern dependence can be established unambiguously only with input waveforms of the same  $\langle i \rangle$ . (In the experimental literature, this rule is not always observed.) Otherwise, pattern dependence may only be inferred, on the basis of assumptions about  $f$ .

**A3.** More formally, our treatment of pattern can be thought of as follows. In most general terms, pattern is, essentially, the waveform  $\mathcal{F}_x$  itself, an infinite-dimensional variable. With our canonical subset of waveforms, we reduce the number of dimensions, in a plausible way, to three:  $F, P$ , and  $\langle i \rangle$ . We then define the pattern  $x$  more strictly in terms of  $F$  and  $P$  only, and to extract its effect from the total effect of  $\mathcal{F}_x$ , we restrict the set of waveforms considered at any one time further so that  $\langle i \rangle$  becomes a constant parameter rather than a variable. More realistically, of course, both pattern and  $\langle i \rangle$  will vary simultaneously. However, the same data that are needed to compute the effect of pattern will also yield that of  $\langle i \rangle$ , and thus the total effect (e.g., Fig. 3 A–C).

**A4.**  $\partial(\mathcal{F}_0) = \langle o \rangle(\mathcal{F}_0)$  is assured as long as  $f$  is time independent, or time dependent only because it has a (decaying) “memory” of the history of  $i$ , as in schema 3. In this paper, we assume that  $f$  has no extraneous time dependence that is not tied in this way to the input waveform.

**A5.** Over the relevant set of  $i$ . Proof along the lines of Eq. 4; we find, of course,  $f = g$ .

**A6.** Most practical cases, of course, will be a matter of approximation:  $\Phi \rightarrow 1$  if the nonlinearity in  $f$  is sufficiently small, the pattern is sufficiently modest ( $F \rightarrow 1$ ) or, when  $f$  is time dependent, its time constant is sufficiently longer than  $P$ .

**A7.** Schema 3 is described by

$$da/dt = \alpha i^p(1 - a) - \beta a; o = a^q. \quad [5]$$

**A8.** The time “constant” varies with  $i$  (see A9). Furthermore, at each  $F$  there are two time constants, for  $i = \langle i \rangle/F$  and  $i = 0$ . For simplicity, we refer to this whole set of related time constants by the generic term “ $\tau$ ”.

**A9.** We solve Eq. 5 in A7, then Eq. 2, for the input waveforms in Fig. 1A. For  $\mathcal{F}_x$  with  $i_x = \langle i \rangle/F$ , in the dynamical steady state of the system,  $a$  cycles from a minimum ( $\underline{a}$ ) to a maximum ( $\bar{a}$ ) along  $a_1(t - t_a) = a_{\infty,x} - (a_{\infty,x} - \underline{a})\exp[-(t - t_a)/\tau_x]$ , where  $\tau_x = (\alpha i_x^p + \beta)^{-1}$  and  $a_{\infty,x} = \alpha i_x^p \tau_x$ , until  $\bar{a} = a_1(FP)$ , then back along  $a_2(t - t_a) = \bar{a} \exp[-\beta(t - t_a)]$  until  $\underline{a} = a_2([1 - F]P)$ .

Combining, we obtain  $\bar{a} = a_{\infty,x}[1 - \exp(-FP/\tau_x)]/\{1 - \exp[-FP/\tau_x - \beta(1 - F)P]\}$  and  $\underline{a} = \bar{a} \exp[-\beta(1 - F)P]$ . For  $\mathcal{J}_0$  with  $i_0 = \langle i \rangle$  and  $F = 1$ ,  $a(t) = \bar{a} = \underline{a} = a_{\infty,0}$ . Then, with all  $a$ 's related to the corresponding  $o$ 's by  $o = a^q$ ,

$$\Phi_{\bar{o}} = \left[ \frac{\bar{a}}{a_{\infty,0}} \right]^q$$

$$= \left[ \frac{\alpha \langle i \rangle^p + \beta}{\alpha \langle i \rangle^p + \beta F^p} \right] \left\{ \frac{1 - \exp[-P(\alpha \langle i \rangle^p F^{1-p} + \beta F)]}{1 - \exp[-P(\alpha \langle i \rangle^p F^{1-p} + \beta)]} \right\}^q, \quad [6]$$

$$\Phi_{\langle o \rangle} = \frac{1}{Pa_{\infty,0}^q} \left( \int_0^{FP} a_1^q dt + \int_0^{(1-F)P} a_2^q dt \right). \quad [7]$$

For any  $q$ , Eq. 7 has a straightforward but lengthy explicit solution, omitted here.

**A10.** From **A9**,  $o_{\infty}(i) = a_{\infty}^q(i) = [\alpha i^p / (\alpha i^p + \beta)]^q$ . Substituting this into the expressions for  $\Phi_{\bar{o}}$  and  $\Phi_{\langle o \rangle}$  in terms of  $o_{\infty}$  in Fig. 2E (and, or taking the limit of Eqs. 6 and 7, as  $P/\tau \rightarrow \infty$ ,  $\Phi_{\bar{o}} \rightarrow [(\alpha \langle i \rangle^p + \beta) / (\alpha \langle i \rangle^p + \beta F^p)]^q$  and  $\Phi_{\langle o \rangle} \rightarrow F \Phi_{\bar{o}}$ ).

**A11.** As  $P/\tau \rightarrow 0$ ,  $o(t) \rightarrow \text{constant}$ , and the steady state may be found simply by equating the time-averaged rates of increase and decrease of  $o$ . Only if the net  $i$ -dependent component of these rates is linear with  $i_x$  is the steady-state  $o = \langle o \rangle$  the same for all  $F i_x = \langle i \rangle$ . In the specific case of schema 3, from Eq. 5 or by taking the limit of Eqs. 6 and 7, as  $P/\tau \rightarrow 0$ ,  $\langle o \rangle \rightarrow [\alpha \langle i \rangle^p / (\alpha \langle i \rangle^p + \beta F^{p-1})]^q$ , and  $\Phi_{\langle o \rangle} \rightarrow [(\alpha \langle i \rangle^p + \beta) / (\alpha \langle i \rangle^p + \beta F^{p-1})]^q$ .

**A12.** That is (decomposing Eq. 5),  $i^* = i^p$ ;  $da/dt - \alpha i^*(1 - a) - \beta a$ ;  $o = a^q$ . How pattern dependence propagates, in general, through such chains or networks of multiple steps is clearly of interest, but beyond the scope of this paper. An important factor is the degree to which the pattern in  $i$  survives the transformation to appear as a pattern in  $o$ . In Fig. 2B, for instance, although  $\Phi_{\bar{o}}$  is the same whether  $P < \tau$  or  $P > \tau$ ,  $o$  is patterned only in the latter case.

**A13.** Since spikes are discrete, firing frequency is not truly a continuous variable. Pattern becomes meaningless when, roughly,  $P < 2/\langle i \rangle$ . However, in the experiments reported in this paper, this limit was sufficiently low not to be a problem. In Figs. 1B and C, and 3C, for example, with mean  $\langle i \rangle = 7$  and 5.7 Hz, the limit was 0.29 and 0.35 s, respectively.

**A14.** The argument in **A11** can be generalized to spectral components of the input waveform with frequencies  $\gg \tau^{-1}$ .

We thank Drs. J. C. Kennedy and L. F. Abbott and the two reviewers for helpful comments. This work was funded by the National Institutes of Health (MH50235, GM320099, K05 MH01427 to K.R.W. and K21 MH00987 to V.B.) and the Whitehall Foundation (to V.B.).

1. Bourque, C. W. (1991) *Trends Neurosci.* **14**, 28–30.
2. Andersson, P.-O., Bloom, S. R., Edwards, A. V. & Järhult, J. (1982) *J. Physiol. (London)* **322**, 469–483.
3. Ip, N. Y. & Zigmond, R. E. (1984) *Nature (London)* **311**, 472–474.
4. Cazalis, M., Dayanithi, G. & Nordmann, J. J. (1985) *J. Physiol. (London)* **369**, 45–60.
5. Birks, R. I. & Isacoff, E. Y. (1988) *J. Physiol. (London)* **402**, 515–532.
6. Peng, Y. & Horn, J. P. (1991) *J. Neurosci.* **11**, 85–95.
7. Whim, M. D. & Lloyd, P. E. (1994) *J. Neurosci.* **14**, 4244–4251.
8. Whim, M. D. & Lloyd, P. E. (1989) *Proc. Natl. Acad. Sci. USA* **86**, 9034–9038.
9. Segundo, J. P., Perkel, D. H. & Moore, G. P. (1966) *Kybernetik* **3**, 67–82.
10. Peng, Y. & Zucker, R. S. (1993) *Neuron* **10**, 465–473.
11. Fields, R. D. & Nelson, P. G. (1993) *J. Neurobiol.* **25**, 281–293.
12. Larson, J. & Lynch, G. (1986) *Science* **232**, 985–988.
13. Grover, L. M. & Teyler, T. J. (1990) *Nature (London)* **347**, 477–479.
14. Markram, H. & Tsodyks, M. (1996) *Nature (London)* **382**, 807–810.
15. Li, M., Jia, M., Fields, R. D. & Nelson, P. G. (1996) *J. Neurophysiol.* **76**, 2595–2607.
16. LeMasson, G., Marder, E. & Abbott, L. F. (1993) *Science* **259**, 1915–1917.

17. Turrigiano, G., Abbott, L. F. & Marder, E. (1994) *Science* **264**, 974–977.
18. Fields, R. D., Neale, E. A. & Nelson, P. G. (1990) *J. Neurosci.* **10**, 2950–2964.
19. Sheng, H. Z., Fields, R. D. & Nelson, P. G. (1993) *J. Neurosci. Res.* **35**, 459–467.
20. Itoh, K., Stevens, B., Schachner, M. & Fields, R. D. (1995) *Science* **270**, 1369–1372.
21. Gillary, H. L. & Kennedy, D. (1969) *J. Neurophysiol.* **32**, 607–612.
22. Stein, R. B. & Parmiggiani, F. (1979) *Brain Res.* **175**, 372–376.
23. Zajac, F. E. & Young, J. L. (1980) *J. Neurophysiol.* **43**, 1206–1220.
24. Bevan, L., Laouris, Y., Reinking, R. M. & Stuart, D. G. (1992) *J. Physiol. (London)* **449**, 85–108.
25. Stevens, E. D. (1996) *J. Physiol. (London)* **494**, 279–285.
26. Cohen, J. L., Weiss, K. R. & Kupfermann, I. (1978) *J. Neurophysiol.* **41**, 157–180.
27. Weiss, K. R., Brezina, V., Cropper, E. C., Heierhorst, J., Hooper, S. L., Probst, W. C., Rosen, S. C., Vilim, F. S. & Kupfermann, I. (1993) *J. Physiol. (Paris)* **87**, 141–151.
28. Brezina, V., Bank, B., Cropper, E. C., Rosen, S., Vilim, F. S., Kupfermann, I. & Weiss, K. R. (1995) *J. Neurophysiol.* **74**, 54–72.
29. Brezina, V., Orekhova, I. V. & Weiss, K. R. (1996) *Science* **273**, 806–810.
30. Goldbeter, A. (1996) *Biochemical Oscillations and Cellular Rhythms* (Cambridge Univ. Press, Cambridge).
31. Hrushesky, W. J. M., Langer, R. & Theeuwes, F., eds. (1991) *Ann. N.Y. Acad. Sci.* **618**.
32. Hodgkin, A. L. & Huxley, A. F. (1952) *J. Physiol. (London)* **117**, 500–544.
33. Colquhoun, D. & Hawkes, A. G. (1977) *Proc. R. Soc. London B* **199**, 231–262.
34. Colquhoun, D. & Hawkes, A. G. (1981) *Proc. R. Soc. London B* **211**, 205–235.
35. Fersht, A. (1977) *Enzyme Structure and Mechanism* (Freeman, San Francisco).
36. Woleged, R. C., Curtin, N. A. & Homsher, E. (1985) *Energetic Aspects of Muscle Contraction* (Academic, London).
37. Kenakin, T. (1993) *Pharmacologic Analysis of Drug-Receptor Interaction* (Raven, New York), 2nd Ed.
38. Gutfreund, H. (1995) *Kinetics For the Life Sciences: Receptors, Transmitters and Catalysts* (Cambridge Univ. Press, Cambridge).
39. Baxter, D. A. & Byrne, J. H. (1993) in *The Neurobiology of Neural Networks*, ed. Gardner, D. (MIT Press, Cambridge, MA), pp. 71–105.
40. Kupfermann, I. & Carew, T. J. (1974) *Behav. Biol.* **12**, 317–337.
41. Pette, D. & Vrbova, G. (1992) *Rev. Physiol. Biochem. Pharmacol.* **120**, 115–202.
42. Holford, N. H. G. & Benet, L. Z. (1995) in *Basic and Clinical Pharmacology*, ed. Katzung, B. G. (Appleton & Lange, Norwalk, CT), 6th Ed., pp. 33–47.
43. Kling, J. W. & Riggs, L. A., eds. (1971) *Woodworth and Schlosberg's Experimental Psychology* (Holt, Rinehart and Winston, New York), 3rd Ed.
44. Kandel, E. R. (1976) *Cellular Basis of Behavior* (Freeman, New York).
45. Berridge, M. J., Rapp, P. E. & Treherne, J. E., eds. (1979) *J. Exp. Biol.* **81**.
46. Rapp, P. E. (1987) *Prog. Neurobiol.* **29**, 261–273.
47. Winfree, A. T. (1990) *The Geometry of Biological Time* (Springer, Berlin).
48. Harris-Warrick, R. M., Marder, E., Selverston, A. I. & Moulins, M., eds. (1992) *Dynamic Biological Networks: The Stomatogastric Nervous System* (MIT Press, Cambridge, MA).
49. Steriade, M., McCormick, D. A. & Sejnowski, T. J. (1993) *Science* **262**, 679–685.
50. Marder, E. & Calabrese, R. L. (1996) *Physiol. Rev.* **76**, 687–717.
51. Laurent, G. (1996) *Trends Neurosci.* **19**, 489–496.
52. Meyer, T. & Stryer, L. (1991) *Annu. Rev. Biophys. Chem.* **20**, 153–174.
53. Petersen, O. H., Petersen, C. C. H. & Kasai, H. (1994) *Annu. Rev. Physiol.* **56**, 297–319.
54. Gu, X. & Spitzer, N. C. (1995) *Nature (London)* **375**, 784–787.
55. Bourne, H. R. & Nicoll, R. (1993) *Cell* **72/Neuron** **10** (Suppl.), 65–75.
56. Hopfield, J. J. (1995) *Nature (London)* **376**, 33–36.
57. König, P., Engel, A. K. & Singer, W. (1996) *Trends Neurosci.* **19**, 130–137.
58. Abbott, L. F. (1994) *Q. Rev. Biophys.* **27**, 291–331.
59. Ferster, D. & Spruston, N. (1995) *Science* **270**, 756–757.
60. Rieke, F., Warland, D., de Ruyter van Steveninck, R. & Bialek, W. (1997) *Spikes: Exploring the Neural Code* (MIT Press, Cambridge, MA).
61. Bygrave, F. L. & Roberts, H. R. (1995) *FASEB J.* **9**, 1297–1303.
62. Ghosh, A. & Greenberg, M. E. (1995) *Science* **268**, 239–247.